On the dynamics of the December 2020 medicane

Gerard Kilroy[a], Hongyan Zhu[b], Minhee Chang[c] and Roger K. Smith[a]*

[a] *Meteorological Institute, Ludwig-Maximilians University, Munich, Germany*
[b] *Research, Science and Innovation, Bureau of Meteorology, Melbourne, Australia*
[c] *School of Earth and Environmental Sciences, Seoul National University, Seoul, South Korea*

*Correspondence to: Prof. Roger Smith, Meteorological Institute, Ludwig-Maximilians University, Munich, Germany. E-mail: roger.smith@lmu.de

A case study of the medicane that formed over the eastern Mediterranean in mid-December 2020 is presented. The study is based on analyses of data from the European Centre for Medium Range Weather Forecasts (ECMWF), imagery from the European geostationary meteorological satellite, Meteosat Second Generation, and output from a convection permitting numerical simulation of the event using the United Kingdom (UK) Met Office regional model with the RAL2 physics configuration. It is shown that the rotating-convection paradigm for tropical cyclone behaviour provides an attractive and consistent framework for interpreting the dynamics of formation and intensification of the medicane. Limitations of the currently widely accepted interpretation invoking the so-called "Wind-Induced Surface Heat Exchange (WISHE) intensification mechanism" are discussed.

Key Words: Tropical cyclone, hurricane, convection, cyclogenesis

Received January 31, 2022; Revised ; Accepted

1. Introduction

From time to time, about 1.6 times per year, small low pressure systems develop over the Mediterranean Sea that have many of the characteristics of tropical cyclones. These characteristics include a warm core structure, an eye-like feature around the centre, strong surface winds with the strongest winds occurring in the eye-wall in the boundary layer and the fact that such storms frequently undergo a rapid intensification phase (Moscatello et al. 2008; von Storch and Gualdi 2014; Cioni et al. 2016). Such systems have acquired the name *medicanes*, short for Mediterranean Hurricanes (Emanuel 2005). Medicanes are often difficult to forecast due to their relative small size and quick intensification phase (Picornell et al. 2014). Excellent up-to-date reviews are given by Michaelides et al. (2018) and Pytharoulis (2018). A recent study of their predictability is provided by Muzio et al. (2019).

Typically, the precursor to medicanes is a large-scale low pressure system that develops first over the Atlantic. This precursor low has a deep cold-core asymmetric structure, which transitions progressively to a shallow warm-core structure once it encounters the warmer waters over the Mediterranean Sea (Cioni et al. 2016). The thermodynamical disequilibrium between the cold core and the warmer waters over the Mediterranean Sea leads to the triggering of deep convective bursts (von Storch and Gualdi 2014).

Like tropical cyclones, the formation of a medicane requires high values of mid-tropospheric relative humidity, relatively low vertical wind shear, high low-level relative vorticity and high values of near surface equivalent potential temperature maintained by surface fluxes in order to keep the environment convectively unstable (Tous and Romero 2013; von Storch and Gualdi 2014). A major difference between the environmental conditions of tropical cyclones and medicanes is that the Mediterranean Sea is much colder than tropical waters. Typically, tropical cyclones do not occur over waters cooler than 26 C, whereas medicanes have been documented forming in waters as cold as 15 C (Tous and Romero 2011). However, in a numerical modelling study, Miglietta et al. (2015) found that medicanes progressively lost their tropical-cyclone-like features, the cooler the sea surface temperatures (SSTs).

Both observational studies (Marra et al. 2019; Miglietta et al. 2011) and numerical studies (Lagouvardos et al. 1999; Pytharoulis et al. 2000; Homar et al. 2003; Carrió et al. 2020) have found persistent deep convection to be a feature of medicanes and an analysis of satellite observations by Dafis et al. (2018) found that medicanes contain deep convective clouds that penetrate into the lower stratosphere, with peak precipitation rates occurring up to 12 hours before the maximum wind speed occurs. In a more recent study, Dafis et al. (2020) used infra-red and microwave satellite diagnostics to study the evolution of deep convection in medicanes that developed between 2005 and 2018, focussing on the role of vertical wind shear in organizing deep convection in these cases.

Notwithstanding the possible effects of vertical wind shear, following the study by Emanuel (2005) a theme of many studies of medicanes has been on the need for surface enthalpy fluxes to support such storms and, like tropical cyclones, the so-called "WISHE

© 2021 Royal Meteorological Society

intensification mechanism" has become entrenched to explain their formation. This is despite the fact that the WISHE mechanism has been long shown to be non-essential to explain tropical cyclone intensification (Montgomery et al. 2009, 2015) and that the underlying theory has been shown to suffer a range of issues (see e.g. Smith et al. 2008, Montgomery and Smith 2017, their Section 5, Montgomery and Smith 2019).

In the last decade, an alternative conceptual model has emerged to explain how tropical cyclones intensify, the so-called rotating-convection paradigm. This paradigm is an extension of the classical axisymmetric theory for intensification discussed by Ooyama (1969). A review of the main paradigms to explain the intensification of tropical cyclones is given by Montgomery and Smith (2014) and a more recent review of the rotating-convection paradigm is provided by Montgomery and Smith (2017). The question then arises as to whether this new paradigm might provide a more useful conceptual framework for understanding the formation of medicanes (but not the parent cyclones within which they develop).

The purpose of the present study is three-fold. The first is to appraise the integrity of the WISHE theory as it has been articulated in the recent medicane literature (Section 2); the second is to present a review of an alternative conceptual framework, the rotating-convection paradigm (Section 3); and the third is to present a case study of the medicane that formed in mid-December 2020 near the island of Cyprus before it crossed the coast of Lebanon on the same day. We will show that the formation and intensification of this event is consistent with the rotating-convection paradigm (Sections 4 to Section 7). The conclusions are presented in Section 8.

2. The WISHE mechanism

Two recent examples suffice to illustrate the entrenchment of the WISHE theory in the context of medicanes. Carrió et al. (2017) write "The accepted conceptual model for the intensification and maintenance of medicanes is similar to that of tropical cyclones, being governed by surface energy fluxes within pre-existing organized cyclonic environments, although with the very substantial difference of the requirement for an upper-level cold trough that contributes to cool and moisten the low and mid-tropospheric environment, thus increasing the air-sea gradient of saturation moist static energy (Emanuel 2005)." Further, in a very recent paper, Miglietta et al. (2020) write "Overall, a general consensus had been reached on how these cyclones intensify in their mature stage*: the so-called wind-induced surface heat exchange (WISHE) theory (Emanuel 1986; Rotunno and Emanuel 1987) suggests that these storms develop in a manner similar to TCs (tropical cyclones, our insertion), as a result of air–sea interaction, and are maintained against dissipation entirely by the energy input from sea-surface fluxes. The vertical motion, associated with atmospheric instability, only redistributes the heat acquired at low levels, such that the eyewall remains close to slantwise moist neutrality (Rotunno and Emanuel 1987)." Miglietta et al. go on to note concerns expressed in two recent papers (Mazza et al. 2017; Fita and Flaounas 2018) about the importance of sea-surface fluxes in two particular case studies, but point out that Miglietta and Rotunno (2019) have "re-analysed the same two cyclones, showing that their intensification cannot be adequately explained without considering sea-surface fluxes and latent heating, in analogy with the WISHE mechanism typical of TCs." It would appear from these papers that the "WISHE mechanism" is alive and well to explain the intensification of medicanes. However, as argued below, we have questions about the integrity of this mechanism.

In view of the fact noted by Montgomery et al. (2015) that there is confusion in the literature on precisely what the WISHE mechanism is, it is pertinent to enquire how the mechanism is articulated in the literature on medicanes. Miglietta and Rotunno (2019) state that all these categories of hybrid Mediterranean cyclones share with tropical cyclones the WISHE mechanism of development in the "tropical-like" part of their lifetime, citing the papers of Emanuel (1986) and Rotunno and Emanuel (1987). First, we note that Emanuel (1986) presents a theoretical model for a steady-state tropical cyclone, not a theory for tropical-cyclone intensification. Further, the study by Rotunno and Emanuel is based on numerical simulations designed to evaluate some of the assumptions made by Emanuel (1986), but fell short of articulating a complete theory for vortex intensification. Their summary on page 559 reads: "We have established, using a numerical model, that a hurricane-like vortex may grow as a result of a finite amplitude instability in an atmosphere which is neutrally stable to the model's moist convection. *The mechanism* (our emphasis), which is a form of air-sea interaction instability, operates in such a way that wind-induced latent heat fluxes from the ocean lead to locally enhanced values of θ_e in the boundary layer which, after being redistributed upward along angular momentum surfaces, lead to temperature perturbations aloft. These temperature perturbations enhance the storm's circulation, which further increases the wind-induced surface fluxes, and so on. The tropical cyclone will continue to intensify so long as boundary-layer processes permit steadily increasing values of θ_e near the core or until the boundary layer there becomes saturated." Here, of course, θ_e refers to the equivalent potential temperature† of the air.

The explanation above begs a number of questions. First, how does a redistribution of locally enhanced values of θ_e in the boundary layer along (absolute) angular momentum surfaces lead to the inward movement of these surfaces, which is a necessary requirement for the tangential velocity component to increase? There must be some dynamics involved here. And how do the "temperature perturbations enhance the storm's circulation"? In the Emanuel (1986) theory, it is assumed that there is no local buoyancy associated with temperature perturbations, i.e. the overturning circulation is moist neutral. None of the papers on medicanes that we have studied that use the term WISHE (including that of Emanuel 2005) have provided a clear articulation of this mechanism. For these reasons, it is not possible to appraise the WISHE mechanism in the December 2020 medicane case to be discussed.

To confuse matters further, Zhang and Emanuel (2016) appear to have redefined the "WISHE feedback process" as simply the formula relating the increase of surface enthalpy flux to the surface wind speed and to the degree of thermodynamic disequilibrium near the surface without explaining how the increased fluxes lead to an increase in surface wind speed as in earlier studies (see e.g. Montgomery and Smith 2014, figure 6 and related discussion). Although section 2 of their paper presents an example of a feedback process, it is unclear how this example relates to the purported WISHE process. The issues are discussed here in Appendix 1.

*This is a curious statement because the mature stage is usually considered to be that in which intensification has ceased.

†Although Emanuel (1986) defines θ_e to be the *reversible* equivalent potential temperature, it was later pointed out by Bryan and Rotunno (2009) on page 3044 that in fact Emanuel had used the *pseudo*-equivalent potential temperature in which all condensate instantaneously rains out. It appears that Miglietta and Rotunno (2019) have reverted to using the reversible definition.

© 2021 Royal Meteorological Society

3. The rotating-convection paradigm

The rotating-convection paradigm considers a cluster of deep convective clouds that persist in a region of sufficient ambient cyclonic rotation over a warm tropical ocean. Collectively, these clouds generate a cluster-scale overturning circulation, the inward branch of which converges absolute vorticity in the lower troposphere. By Stokes' theorem, this convergence leads to an amplification of the mean tangential velocity at a given radius from the centre of the cluster. In the divergent branch of the circulation in the upper troposphere, absolute vorticity is advected away from the centre whereupon the tangential velocity component spins down and even reverses sign beyond a certain radius.

The persistence of deep convection over a period of days requires a sufficient moisture supply from the ocean to maintain convective instability and is assisted by a progressive local moistening of the troposphere within the cluster through the evaporation of previous clouds (e. g., Nolan 2007, Kilroy et al. 2017b, Figure 8c). This moistening reduces the strength of convective downdraughts that would otherwise lead to convective stabilization (e.g. Emanuel 1986). Moreover, the elevation of near-surface moisture increases the buoyancy of cloud updraughts, thereby strengthening the cluster-scale overturning circulation. The local amplification of vorticity within deep convection is a prominent feature of vortex evolution also and the stochastic nature of the convection introduces a stochastic element to the evolution of the vorticity field.

In an azimuthally-averaged perspective, the rotating-convection paradigm includes, but extends, the classical axisymmetric paradigm for vortex intensification articulated by Ooyama (1969). In this paradigm, inflow in the lower troposphere induced by deep convection within the vortex circulation is argued to draw absolute angular momentum surfaces inwards. Above the frictional boundary layer, absolute angular momentum, M, is approximately materially conserved so that the inward movement of these surfaces implies a local spin up of the tangential velocity component. The extension invokes a boundary-layer spin up mechanism to explain the observed occurrence of the maximum tangential winds in the tropical cyclone boundary layer and accounts for both azimuthal mean and eddy contributions to the dynamics and thermodynamics of vortex spin up (Persing et al. 2013; Smith et al. 2017; Montgomery et al. 2020).

There is ample evidence from prior studies of medicanes to suggest that the rotating-convection paradigm could provide a useful conceptual framework for understanding their dynamics, especially for the case to be presented in which ambient vertical shear appears to be minimal. This conceptual framework would be attractive as it would defuse the intense debate in the medicane literature on the role of surface enthalpy fluxes in medicane formation. Notwithstanding the fact that some studies have played down the role of surface enthalpy fluxes in medicane formation (e.g. Carrió et al. 2017), the statement by Homar et al. (2003) that the latent-heat flux is crucial for cyclogenesis, helping to maintain the development of deep convection, is worthy of note. The requirement of some elevated surface enthalpy flux to maintain deep convection is in line with the rotating-convection paradigm, althought this flux is not required to increase with wind speed as in the original WISHE theory.

Even if, as indicated by the analyses of Dafis et al. (2020), significant vertical shear is often a prominent feature of medicanes, the rotating-convection paradigm may still be applicable with some modification. An example of its application to the rapid intensification of Atlantic Hurricane Earl (2010) is presented by Smith et al. (2017).

4. Data sources for the case study

The case study of the December 2020 medicane is based on three data sets: ECMWF analyses, satellite imagery and a high-resolution convection-permitting simulation as described below.

4.1. ECMWF analyses

The ECMWF analysis data are available at 6-hourly intervals on standard vertical pressure surfaces with a horizontal grid spacing 0.125^o longitude $\times 0.125^o$ latitude. The data are available at 25 pressure levels starting at 1000 mb and ending at 1 mb.

4.2. Satellite data

Satellite imagery is available from the geostationary Meteosat Second Generation (MSG) satellite (Schmetz et al. 2002). In order to highlight the location of deep convection, we use the Spinning Enhanced Visible and Infra-red Imager (SEVIRI) instrument on board this satellite. From this instrument, the brightness temperatures derived from infra-red (IR; centre wavelength of 10.8 μm) and water vapour (WV; centre wavelength of 6.25 μm) measurements are obtained with 3 km pixel resolution. The location of deep convection is determined by taking the difference between two brightness temperatures (IR minus WV) using the algorithm employed by Olander and Velden (2009).

4.3. The Met Office regional model simulation

The forecasts are carried out using the convection-permitting regional model with the RAL2 physics configuration developed at the UK Met Office, henceforth known as the Met Office regional model. A summary of the model with references is given in Appendix 2. The model is integrated for 48 hours with the initial condition downscaled from the driving Met Office global model at 0300 UTC on 15 December 2020. The model nominal horizontal grid spacing is 0.036^o in latitude and longitude and there are 90 vertical levels. The main feature to note is that the model is convection permitting: that is, deep convection is represented explicitly and not parametrized. The horizontal domain runs from approximately 10^oE to 50^oE longitude and from 15^oN to 55^oN latitude with output data stored every hour.

© 2021 Royal Meteorological Society

5. Analyzed structure

Figure 1 shows the evolution of mean sea level pressure in the ECMWF analyses from 00 UTC 14 December to 18 UTC 16 December, focussing mainly on the 18 hour period starting at 00 UTC 16 December. The precursor disturbance was a low that was present over the western Mediterranean many days earlier. From 00 UTC 14 December, the low tracked east-southeastwards and later on 15 December began tracking northeastwards. From 00 UTC 15 December, the precursor disturbance progressively filled. The filling is indicated in Figure 1 by a shrinking of the region of blue isobars with values less than 1010 mb. The medicane of interest developed rapidly on 16 December when the low centre was just to the east of Cyprus and it decayed later that day as it crossed the coast of Lebanon.

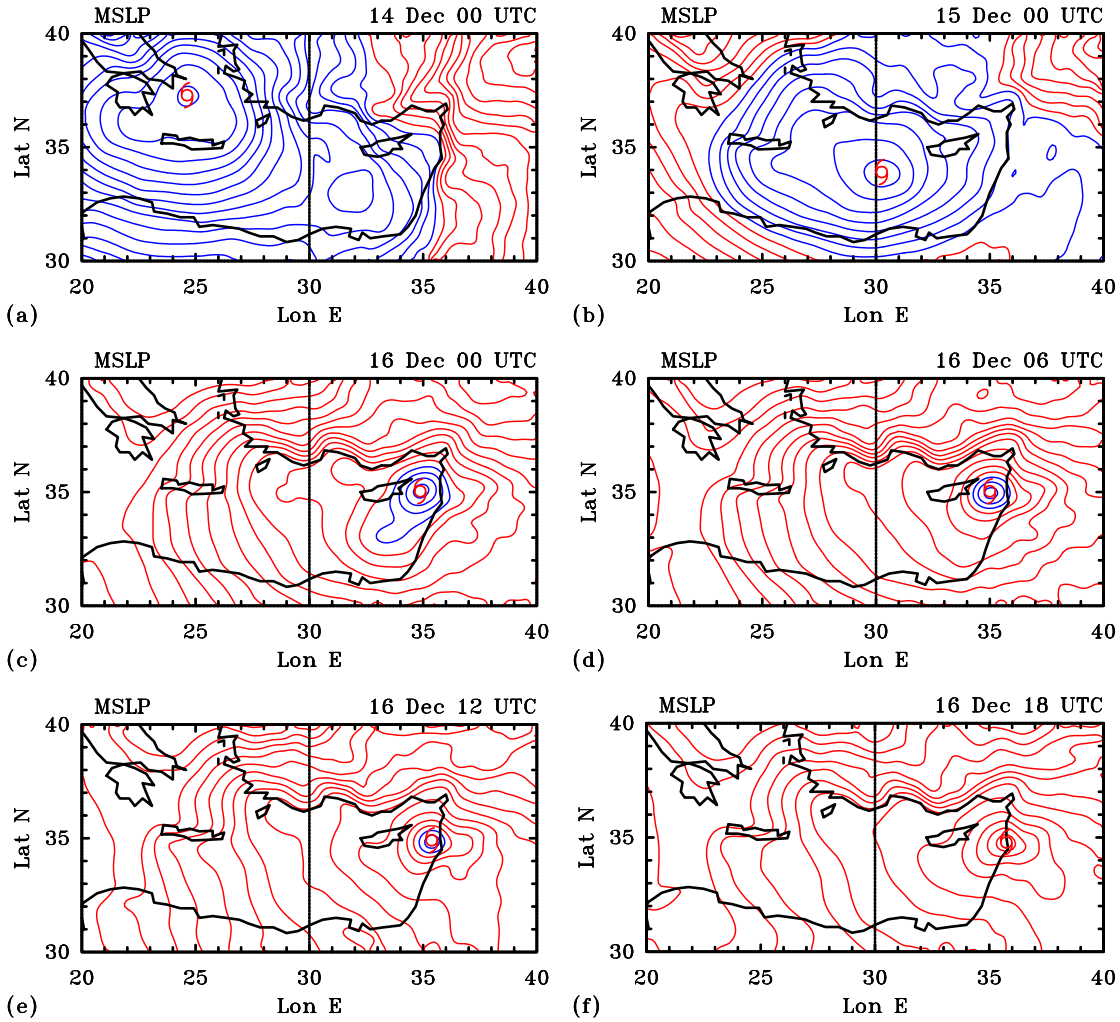

Figure 1. ECMWF mean sea level pressure analyses for 00 UTC on (a) 14 December, (b) 15 December, (c) 16 December and at (d) 06 UTC, (e) 12 UTC and (f) 18 UTC on 16 December 2020. Contour interval 1 mb. Blue isobars for pressures $\leq$ 1010 mb, red isobars for higher pressures.

Because of the progressive filling of the broader-scale parent low, the development of the medicane is barely noticeable in a time-series of minimum surface pressure, being merely a brief flattening out of the curve. On the other hand, the development is more pronounced in sequences of zonal (and meridional) cross sections of pressure through the temporally varying location of the minimum pressure. As an alternative to plotting a whole sequence of such curves, we show in Figure 2 a Hovmöller diagram constructed from these cross sections.

The development of the medicane is seen as an upward-pointing nose of relatively low pressure, below 1010 mb, at longitudes between about 33^{o}E and 36^{o}E that begins to develop at about 21 UTC 15 December and lasts for about a day. Despite the generally rising pressures at all longitudes, the medicane is highlighted by a local strengthening of the zonal pressure gradient on either side of the pressure minimum.

5.1. Track and intensity

Figure 3 shows the location of minimum surface pressure from the ECMWF analyses and from the Met Office regional model simulation. The centre locations on 16 December at 00, 06, 12 and 18 UTC are listed in Table 1. There is a good agreement between the two sets of centre locations on 16 December with the development of the medicane with errors being mostly within half a degree or less.

As a simple measure of intensity, we show in Fig. 4 the time evolution of maximum near-surface (10 m) wind speed (V_{max}) within a radius of 150 km from the minimum wind speed,[‡] and the radial distance of this maximum (r_{Vmax}) from the centre of circulation

[‡]The minimum wind speed was arbitrarily constrained to lie within about 0.5 deg latitude of the location of minimum geopotential height at 850 mb. These locations converged as the storm intensified.

© 2021 Royal Meteorological Society

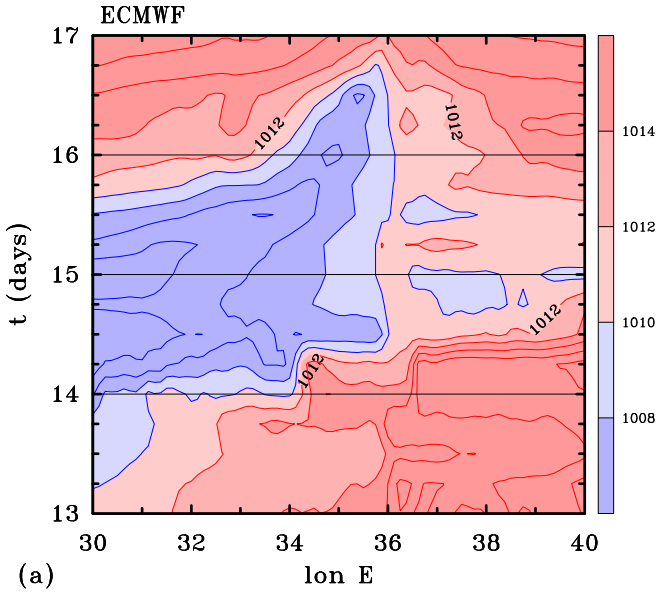

Figure 2. Hovmöller diagram of zonal cross sections of mean sea level pressure through the minimum pressure in the ECMWF analyses for the period 00 UTC 13 December to 00 UTC 17 December 2020. Contour interval 2 mb. Colour shading levels indicated on the side bar.

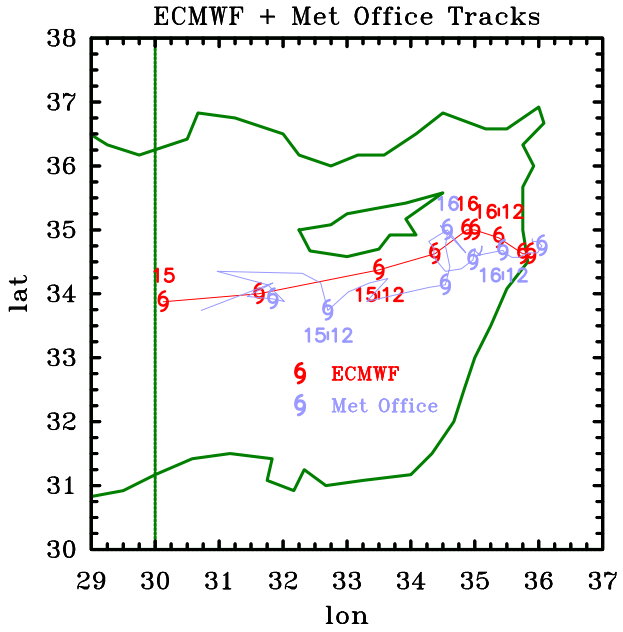

Figure 3. Locations of minimum mean sea level pressure of the low between 00 UTC 15 December and 00 UTC 18 December in the ECMWF analyses (red cyclone symbols) and from the Met Office regional model simulation (blue symbols) that will be discussed in Section 6. The track of the simulation is based on 1 hourly output data. Dates and times every 12 hours for each data set are indicated.

Table 1. Comparison of centre locations (minimum mean sea level pressure) in the ECMWF analyses and in the Met Office regional model simulation on 16 December 2020 at times indicated.

	00 UTC		06 UTC		12 UTC		18 UTC	
	lon	lat	lon	lat	lon	lat	lon	lat
ECMWF	34.875	35.000	35.000	35.000	35.375	34.875	35.750	34.625
Met Office	34.570	35.000	34.970	34.530	35.440	34.680	36.050	34.750

in the ECMWF analyses and the Met Office regional model simulation. In the ECMWF analyses, the medicane just reached tropical storm strength at 00 UTC 16 December, but the strongest 10 m wind speed at this time occurred at a radius of about 70 km (Fig. 4b) while the vortex was still contracting. In the higher-resolution Met Office regional model simulation, the 10 m maximum wind speed increased rapidly from about 15 m s^{-1} at the initial time (03 UTC 15 December) to 23 m s^{-1} at 18 UTC 15 December. Thereafter, the intensity remained above 20 m s^{-1}, i.e., above tropical storm strength, until 21 UTC 16 December. The systematic vortex contraction in the forecast is more easily seen in the azimuthally averaged tangential wind speed shown in Fig, 7b because the radial location of maximum 10 m wind speed fluctuates each hour on account of local outbreaks of deep convection.

© 2021 Royal Meteorological Society

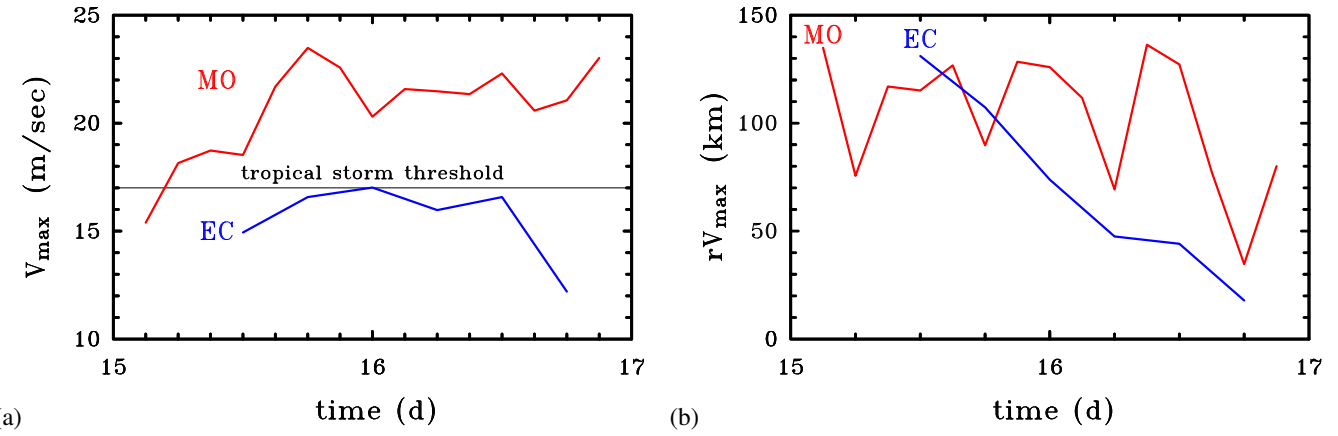

Figure 4. Time evolution of (a) maximum near-surface (10 m) wind speed (V_{max}) within a radius of 150 km from the minimum wind speed, and (b) the radial distance of this maximum ($r_{V\,max}$) from the centre of circulation in the ECMWF analyses (marked EC) and the Met Office regional model simulation (marked MO).

5.2. Vorticity and vertical velocity structure

The upper panels of Figures 5 and 6 show longitude-latitude cross sections of winds, geopotential and absolute vorticity at 850 mb from the ECMWF analyses at six hour intervals starting from 00 UTC 16 December. Super-imposed on these cross sections are contours of 20 cm s^{-1} vertical velocity at 500 mb, which provide an indication of the location of regions of deep convection in the analyses. Recall that deep convection in the analyses is based on parametrized convection in the underlying ECMWF forecast-analysis system and is not expected to correspond accurately with the location of deep convection that was observed. Nor, of course, does the magnitude of vertical motion in the analyses reflect the actual vertical velocities in deep convective updraughts, which are much larger.

The middle panels of these Figures 5 and 6 show the corresponding infra-red satellite imagery and will be discussed in the next subsection. The lower panels of these figures show similar fields to those in the upper panels, but taken from the Met Office regional model simulation. These panels will be discussed in detail in Section 6.

The ECMWF analyses show a core of cyclonic absolute vorticity centred on the location of minimum surface pressure (marked by a cyclone symbol) and between 1 and 2 degrees in diameter[§]. This vorticity core is the remnant of a much broader core that was associated with the precursor low (not shown) and the medicane forms within this region of enhanced vorticity.

Significantly, at each time shown, there are areas of deep convection over the core of enhanced vorticity, some of which are close to, or straddle, the location of minimum surface pressure. In turn, this centre is close to the centre of vortex circulation. These features are similar to those found in developing tropical lows in the Australian region (Smith et al. 2015; Kilroy et al. 2016b, 2017a; Zhu and Smith 2020) and of some medicanes (Dafis et al. 2020, e.g., section 5). As explained in Section 3, the presence of deep convection near the centre of a pre-existing circulation is a central feature of the rotating-convection paradigm, which calls for the overturning circulation associated with the collective effects of deep convection to converge absolute vorticity, thereby increasing the vortex circulation. We explore the azimuthally-averaged aspects of this basic intensification process using the Met Office simulation in Section 6.1.

5.3. Satellite imagery

The middle panels of Figures 5 and 6 show the processed satellite imagery from the MSG satellite described in Section 4.2, which provide the main observational data for the medicane as there appear to be no in situ observations over the sea.

At 00 UTC 16 December (Figure 5c), the main features are the patch of cirrus clouds extending approximately northeastwards from the island of Cyprus, the smaller patch just west of Cyprus and the more linear band extending southwest to northeast mostly over land, covering most of Lebanon and a part of western Syria. Overall, the pattern of this cirrus presents cyclonic circulation with its center roughly coincides with the minimum sea-level pressure in the ECMWF analysis. The region of cirrus cloud northeast of Cyprus shows some small patches of deep convective cells (the pink areas) with one patch just to the northeast of the minimum sea-level pressure in the ECMWF analysis. As expected, these cells do not coincide with the localized updraughts in the ECMWF analysis, but the analyses do show updraught cells in the vicinity of the cells observed.

At 06 UTC 16 December (Figure 5d), there is an almost circular cirrus shield to the east of Cyprus with deep convection at its centre. There are some updraught cells in the ECMWF analysis on the periphery of the circular cirrus shield in the south to west sector, but the linear band just west of the coast remains a feature of the analysis. This band would need to be displaced 1-2 degrees eastwards to line up approximately with regions of observed cirrus (Figure 5b). Nevertheless, the circular cirrus shield closely coincides with the low seen in the geopotential height contours and the deep convection at its centre is just to the north of the minimum geopotential height at 850 mb, which in turn is the location of minimum sea-level pressure in the ECMWF analysis. As shown later, the vortex axis is close to vertical through much of the troposphere, an indication that vertical wind shear is not appreciable.

At both 12 UTC and 18 UTC 16 December (Figures 6c and 6d, respectively), the cirrus shield remains centred close to the location of minimum sea-level pressure in the ECMWF analysis. Deep convection persists within the shield, but is now located a little to the east of the minimum sea-level pressure in the ECMWF analysis.

In summary, the satellite observations show that deep convection persists within the area of cirrus overcast during the 18 hour period of the medicane and some of this convection is located well within the circulation found in the ECMWF analyses. In particular, there are times when the observed convection is at or relatively close to the analysed circulation centre.

[§]Note at latitude 35°N, the central latitude shown in Figures 5 and 6, 1 degree of longitude is only 91 km, whereas 1 degree of latitude is 111 km so that purely circular features would be distorted in a longitude-latitude depiction.

© 2021 Royal Meteorological Society

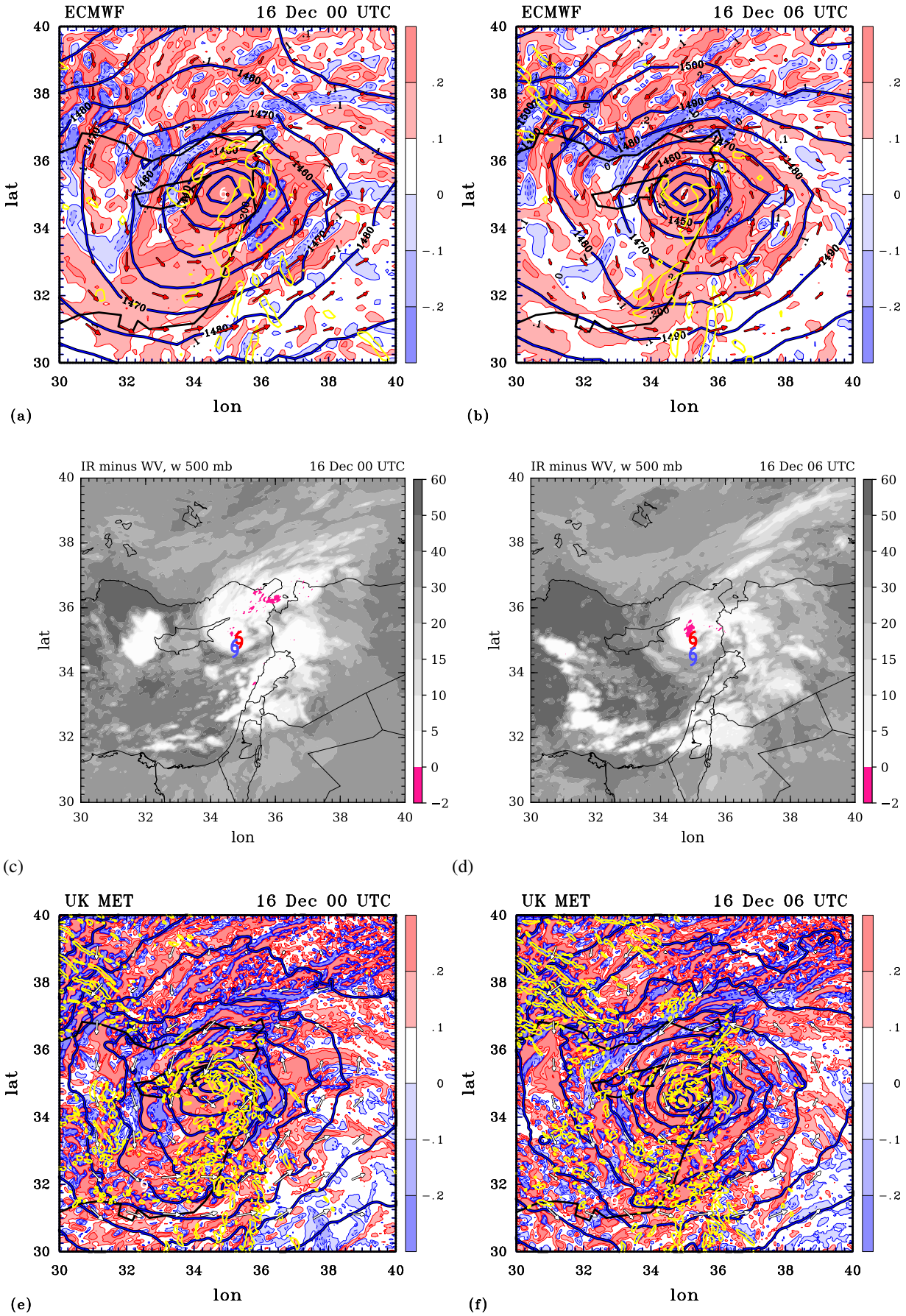

Figure 5. Longitude-latitude cross sections of wind vectors, geopotential (Z, units m) and absolute vorticity (shaded) at 850 mb from the ECMWF analyses (upper panels) and the Met Office regional model simulation (lower panels) at 00 UTC 16 December (left panels) and 06 UTC 16 December (right panels). Super-imposed on these cross-sections are contour of 20 cm s^{-1} vertical velocity at 500 mb. The middle panels show the corresponding Meteosat brightness temperature difference between the infra-red and water vapour channels (shadings, K) at this time. Locations of minimum mean sea level pressure of the low in the ECMWF analyses (red cyclone symbols) are shown in this panel. Contour intervals in the upper and lower panels: 10 m for Z; 1×10^{-3} for ζ, positive contours solid, negative contours dashed, colour shading levels on the side bar.

© 2021 Royal Meteorological Society

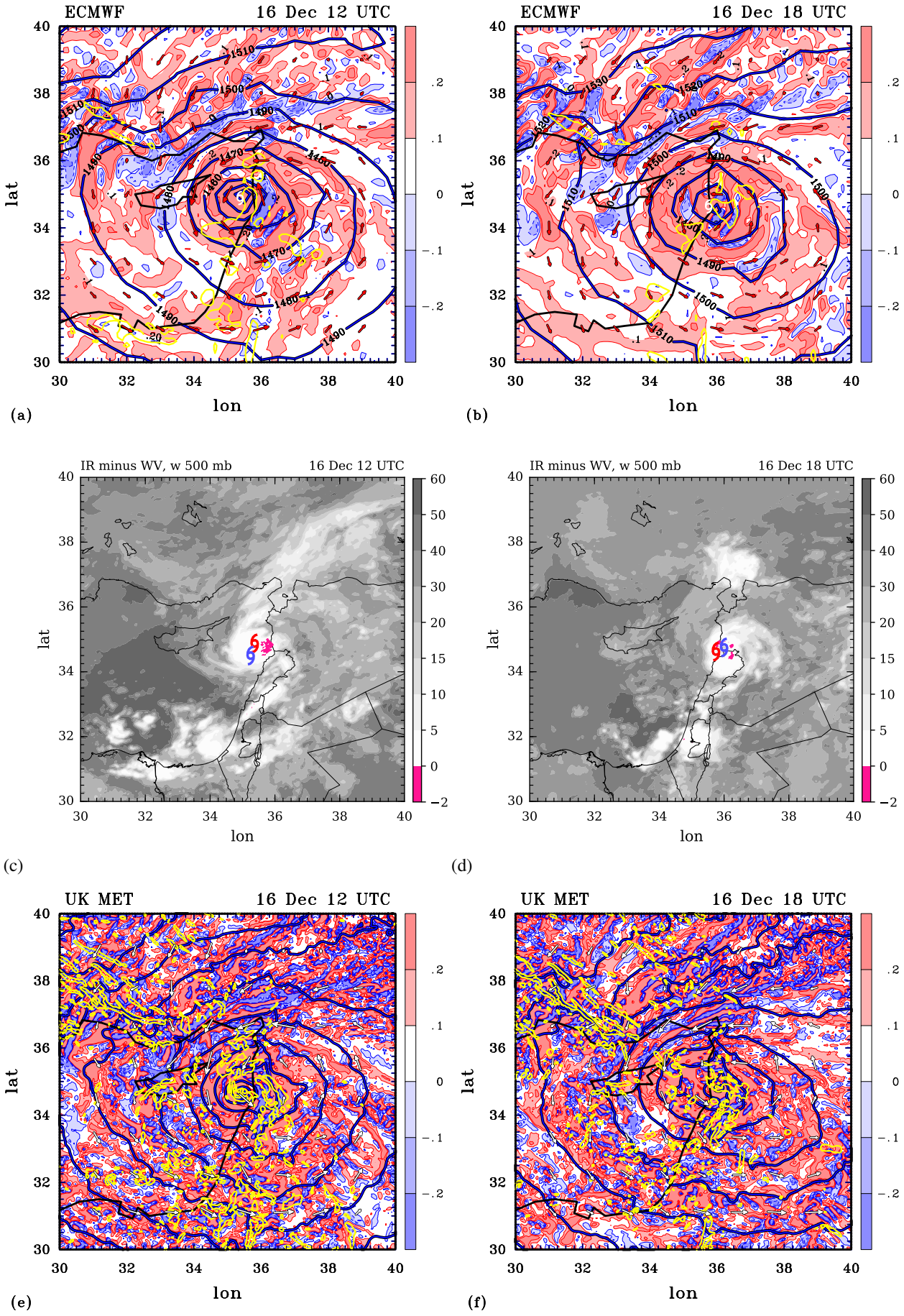

Figure 6. Legend as for Figure 5, but for 12 UTC 16 December (left panels) and 18 UTC 16 December (right panels).

5.4. Vertical structure

Figure 7 shows vertical cross sections of the medicane relative meridional wind component as a function of longitude and height, and the medicane relative zonal wind component as a function of latitude and height, together with the isentropes of potential temperature

© 2021 Royal Meteorological Society

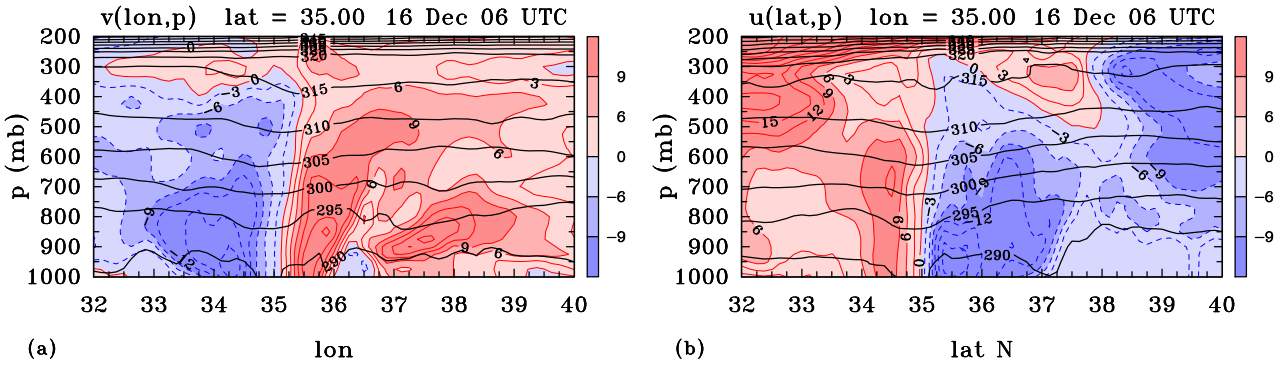

Figure 7. Vertical cross sections of (a) the relative meridional wind component, v_r, as a function of longitude and height, and (b) the relative zonal wind component, u_r, as a function of latitude and height from the ECMWF analysis at 06 UTC 16 December. Superimposed on both panels are the isentropes, θ. Contour interval 3 m s^{-1} for u and v, positive values red, solid, negative values blue, dashed. Contour interval is 5 K for θ. Shading levels on the side bar.

from the ECMWF analysis at 06 UTC 16 December. At this time, the medicane was moving relatively slowly with velocity components 1.35 m s^{-1} to the east and 0.58 m s^{-1} to the south. Three features are particularly noteworthy. First, the relative vortical flow normal to the cross section is a maximum at a height below the 900 mb pressure level, i.e. below 1 km, but only on the northern and western sides of the vortex. Second, the rotation axis has little tilt with height, particularly at heights below the 700 mb pressure level, which, as noted earlier, is an indication that vertical wind shear is not a major factor of the development. Third, the isentropes dip down at along the vortex axis indicating that the vortex is warm cored. Moreover, the warming is largest where the vortical winds are strongest. The situation is similar at other times during the evolution on 16 December (not shown) and such features are similar to those found in tropical cyclones, although in these generally more intense systems, the warming tends to be largest in the upper troposphere.

6. The Met Office regional model simulation

The lower panels of Figures 5 and 6 show the same fields as in the upper panels, but for the Met Office regional model simulation. Because of the somewhat finer grid spacing (0.036^o compared with 0.125^o for the ECMWF analyses), the fields exhibit more fine structure, but the principal features are much the same as in the ECMWF analyses. The geopotential height fields are quite similar as is the location of minimum surface pressure (see Table 1 for details), but the minimum geopotential height is slightly lower in the forecast, again presumably because of the finer horizontal resolution.

The area enclosed by the 20 cm s^{-1} contours of vertical velocity is considerably more extensive than in the two analyses, a feature that is attributable to the higher horizontal resolution of the forecast and the fact that convection is determined explicitly and not based on a parametrization as in the analyses. The absolute vorticity field is broadly similar except that cyclonic vorticity is punctuated more by fine-scale negative absolute vorticity, presumably a result of the finer structures of deep convection (Chagnon and Gray 2009; Kilroy et al. 2014; Weijenborg et al. 2017). The better resolved vertical velocity gradients lead also to a higher magnitude vorticity tendency from tilting.

Note that the forecast for 00 UTC on 16 December has a line of convective cells just offshore of the Mediterranean east coast (Figure 5e), much as in the ECMWF analysis (Figure 5a). However, it has also several deep convective cells close to the vortex centre to the east and north. At both 06 UTC (Figure 6c) and 12 UTC (Figure 7c), deep convection continues to prevail at and surrounding the vortex centre and it is present at the centre and in the northern half of the vortex even at 18 UTC when the centre has just moved over land (Figure 8c). Of course, because deep convective cells have lifetimes much less than the 6 hour interval between the foregoing analyses times and because of their stochastic nature, a more detailed temporal analysis of deep convection in relation to the circulation centre is called for. Such an analysis will be a topic for Section 6.1.

6.1. Azimuthally averaged fields

Because the features of deep convection in the regional model are likely to be more realistic (at least in a statistical sense) than those of the two analysis systems, we use the Met Office regional model simulation to demonstrate the applicability of the rotating-convection paradigm to understanding the dynamics of the December 2020 medicane. To this end we show in Figure 8 selected azimuthally averaged fields centred at the location of minimum wind speed[¶] within the low circulation at 850 mb. These averages, calculated from hourly model output from 03 UTC 15 December to 00 UTC 17 December, are constructed as follows. Data from the latitude-longitude grid-points in the model are mapped on to a Cartesian grid (x, y) with the origin at $(0, 0)$ using distances and angles calculated along great circles on the approximately spherical earth. The new grid is irregular and rather than interpolating to a regular grid, we assign the data points to annular regions with 10 km in radial extent to a radius of 150 km. The data in each annulus are then averaged to provide an azimuthal average nominally at points from 5 km to 145 km at intervals of 10 km. Hovmöller diagrams of the average fields shown in Figure 8 include the vertical velocity at 500 mb, the radial and tangential velocity at 850 mb, which is a little above the frictional boundary layer, the absolute angular momentum, M, at this level, and the radial velocity at 950 mb, which is within the boundary layer. The absolute angular momentum is constructed from the tangential velocity with the assumption of a mean value of Coriolis parameter corresponding to a latitude of 35^o, close to the latitude of the low centre.

Figure 8a shows the vertical velocity at 500 mb. For much of the time period shown, there is mostly ascent within the circle of radius 150 km with bursts of deep convection evident even in the azimuthal mean from about midday on 15 December until about 18 UTC on

[¶]These locations are within 0.25^o latitude of the location of minimum geopotential.

© 2021 Royal Meteorological Society

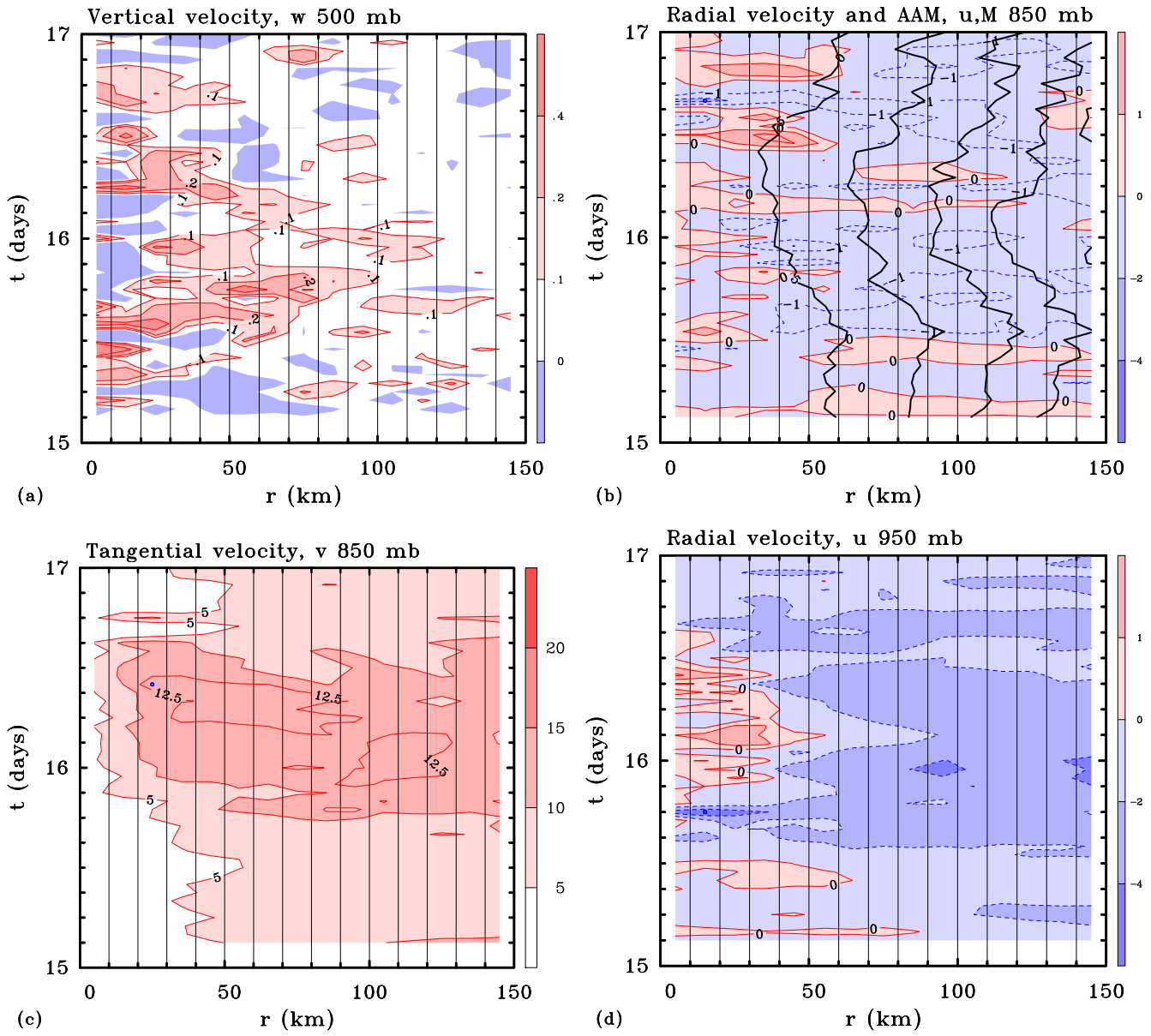

Figure 8. Hovmöller diagrams of selected azimuthally averaged velocity components at selected levels based on the Met Office regional model forecast. These averages are constructed in annular regions each of width 10 km: (a) vertical velocity at 500 mb, (b) radial velocity u (shaded) and absolute angular momentum M (contours) at 850 mb, (c) tangential velocity at 850 mb, and (d) radial velocity at 950 mb from 03 UTC 15 December to 00 UTC 17 December 2020. Contour intervals: (a) 0.1 m s^{-1}; (b) for $u \geq -1$ m s^{-1} the interval is 1 m s^{-1}, for $u < -1$ m s^{-1} the interval is 2 m s^{-1}, for M 5×10^5 m^2 s^{-1}; (c) 5 m s^{-1} with one extra contour of 12.5 m s^{-1}, (d) for $u > 0$ m s^{-1}, the interval is 1 m s^{-1}, for $u < 0$ m s^{-1}, the interval is 2 m s^{-1}. Positive contours red solid curves, negative contours blue dashed curves. Shading values on the side bar. The small blue circle in panel (c) indicates the time and location of the maximum tangential wind.

16 December, several of them occurring in the innermost 10 km region. Over much of the period after 06 UTC 15 December there is inflow at 850 mb at most radii beyond about 50 km, with a few pulses of weak outward flow at specific times (Figure 8b). Such outward pulses are to be expected when, at a particular time, the inflow in the boundary layer is too strong to be fully ventilated by inner-core deep convection (Kilroy et al. 2016a; Smith et al. 2021). The movement of the M-surfaces is generally inwards between 12 UTC on the 15th to 12 UTC on the 16th, except in regions of radial outflow, consistent with the approximate[‖] conservation of M at this level.

Figure 8c shows the evolution of the azimuthally averaged tangential velocity at 850 mb. While there is a general increase at all radii until about 10 UTC 16 December, the maximum tangential wind at that time is 13.9 m s^{-1} and it occurs at radius of about 24 km, indicating a much weaker vortex than a typical tropical cyclone. This may be a reflection of the relatively short time period available for growth before the vortex became strongly influenced by the east coast of the Mediterranean.

Figure 8d shows the evolution of the azimuthally averaged radial velocity at 950 mb. The inflow is much stronger and more extensive than at 850 mb with maximum values in excess of 4 m s^{-1}, reflecting the dominance of frictionally-induced inflow.

Figure 9 shows the evolution of the azimuthally averaged radial and tangential velocity components at 1000 mb, typically a few 10's of metres above the surface. The radial inflow is mostly a little larger than at 950 mb consistent with boundary layer theory. The maximum tangential wind speed at 1000 mb is larger than that at 850 mb, but occurs at a similar radius, around 25 km (Figure 9b) indicating strong spin up in the friction layer. In fact, the tangential wind speeds are a larger still at 950 mb (not shown). This seemingly paradoxical result is a consequence of the boundary layer spin up mechanism articulated by Smith et al. (2009) in the context of tropical cyclones. This mechanism may be understood as follows.

[‖] And the fact that the vertical advection of M is small at this level compared with the radial advection of M.

© 2021 Royal Meteorological Society

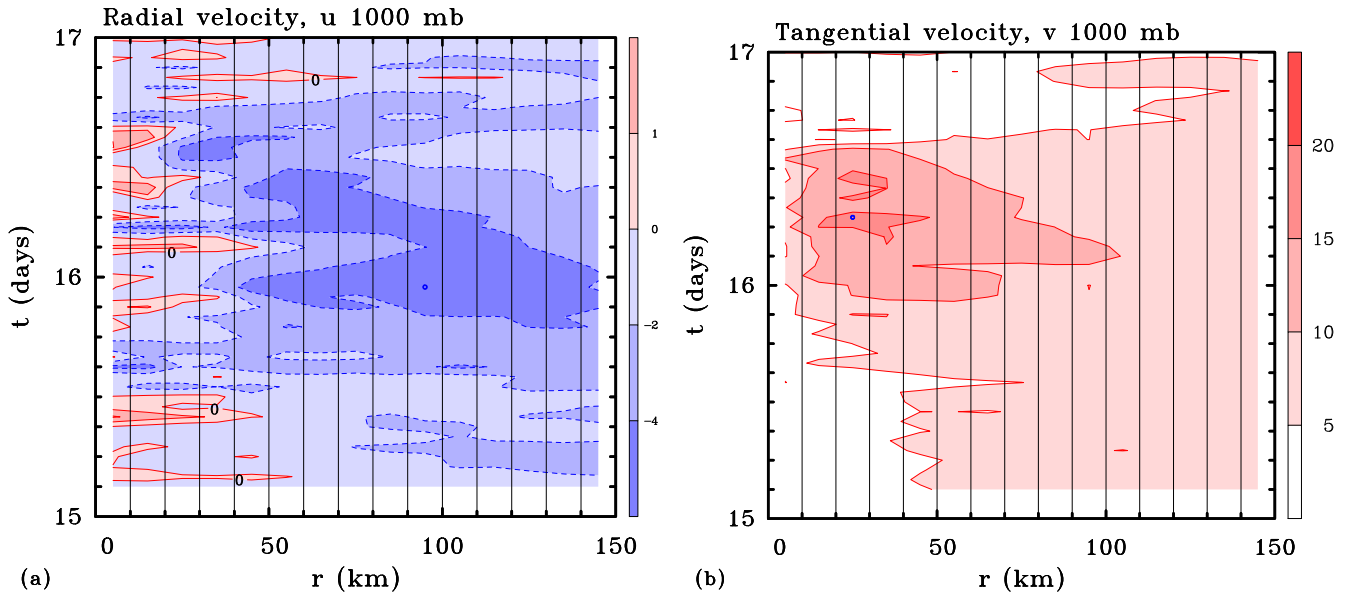

Figure 9. Hovmöller diagrams of azimuthally averaged (a) radial velocity u and (b) tangential velocity v components at 1000 mb from 03 UTC 15 December to 00 UTC 17 December 2020 based on the Met Office regional model simulation. Contour intervals: for $u > 0$ m s^{-1} the interval is 1 m s^{-1}, for $u < 0$ m s^{-1} the interval is 2 m s^{-1}; for v 5 m s^{-1}. Positive contours red solid curves, negative contours blue dashed curves. Colour shading values on the side bar. The small blue circle in panel (b) indicates the time and location of the maximum tangential wind.

Above the boundary layer, absolute angular momentum is approximately materially conserved and since $v = M/r - \frac{1}{2}rf$, as the radius of an inward-moving air parcel decreases, v must increase. In the boundary layer, M is reduced by friction so that for an inward-moving air parcel, both M and r decrease, but if M decreases less rapidly than r, v will still increase. Now M decreases because of the frictional torque on the tangential wind speed. At large radii, air parcels trajectories have a large circular component and radial inflow velocities are comparatively small so that the rate of decrease of M per unit radial displacement of the air parcel is comparatively large. On the other hand, at smaller radii where inflow velocities tend to be larger and parcel trajectories smaller in circumference, the rate of decrease of M per unit radial displacement might conceivably be less than the rate of decrease in r. In essence, the boundary layer spin up mechanism refers to this scenario and provides an explanation for the finding that the maximum tangential wind speed observed in a tropical cyclone occurs within the frictional boundary layer. It provides also an explanation for the observed occurrence of supergradient winds in the tropical cyclone boundary layer and in numerical simulations of tropical cyclones.

7. Interpretations

Taken together, the evolution of vorticity and deep convection discussed in Sections 5.2 and the azimuthally-averaged fields presented in Section 6.1 support the applicability of the rotating-convection paradigm as a framework for understanding the dynamics of the December 2020 medicane. The intensification of the medicane is similar to that in the idealized tropical cyclogenesis simulations of Kilroy et al. (2017b) and Kilroy et al. (2018), whereby deep convection forms near the centre of a weaker existing circulation and generates an overturning circulation that converges absolute vorticity in the lower troposphere, thereby, according to Stokes' circulation theorem, increasing the circulation around fixed closed circuits surrounding the axis. This is essentially the classical mechanism for tropical cyclone intensification articulated by Ooyama (1969), but phrased in terms of vertical vorticity. In an axisymmetric vortex such as used by Ooyama, the analogy would be of the overturning circulation drawing the surfaces of absolute angular momentum, M, inwards with M being materially conserved above a shallow frictional boundary layer**.

Imagine an isolated deep convective cell at some distance from the rotation axis. Clearly, the closer the cell to the circulation centre, the more geometrically favourable is its location for concentrating absolute vorticity (Smith and Montgomery 2016), since cell will produce the low-level inflow only at radii larger than the radius of the cell. At smaller radii, the cell will produce low-level outflow. This idea is supported by statistical analyses of airborne Doppler radar observations of Atlantic hurricanes by Rogers et al. (2013), who found that in rapidly intensifying storms, there is a tendency for vigorous deep convective busts to occur inside the radius of maximum tangential winds.

The azumuthally averaged fields provide a zero order picture of the dynamics, showing that the dynamics are consistent with Ooyama's classical theory for tropical cyclone intensification and its extensions that are part of the rotating-convection paradigm. In particular, they support the role of the boundary layer spin up mechanism in generating the maximum tangential wind speed in the near-surface friction layer.

** Since the tangential wind v_θ and M are related by the formula $v = M/r - \frac{1}{2}fr$, r being the radius and is f the Coriolis parameter, the materially conservation of M implies that v_θ will increase as r decreases.

© 2021 Royal Meteorological Society

8. Summary and Conclusions

We have presented a case study of a medicane that formed in mid-December 2020 near the island of Cyprus. The study is based on several data sets including ECMWF analyses, Meteosat satellite imagery and a convection-permitting numerical simulation using the Met Office regional model.

The medicane developed within a precursor larger-scale low that was active over the western Mediterranean many days earlier, but which was filling at the time of medicane formation. On 16 December the medicane developed rapidly just to the east of Cyprus, and decayed rapidly within 24 hours of formation as it made landfall on the coast of Lebanon. The medicane was captured consistently by the analyses and by the Met Office regional model simulation with the location of minimum surface pressure differing by no more than about 0.25^o degrees latitude at any particular time. This location was close to the location that might be inferred from the satellite images. Of course, with higher horizontal resolution, the features become progressively less smooth with those in the ECMWF analyses being much smoother than those in the Met Office simulation. Overall, these findings add a degree of confidence to using the analysis data set or the forecast for investigating the medicane structure.

In its mature stage, the vortex had a warm core structure with maximum relative tangential flow below the 900 mb pressure level, i.e. below 1 km. The rotation axis had little tilt with height, particularly at heights below the 700 mb pressure level, an indication that vertical wind shear is not appreciable. These are features in common with tropical cyclones in a weakly vertically-sheared environment.

Analyses of the various data indicate that the formation and intensification of this event may be understood in the context of the rotating-convection paradigm. Satellite observations and both analysis and forecast data indicate that during the formation and intensification stages, areas of deep convection are located close to the existing core of enhanced vorticity around the vortex centre, as is the case with tropical cyclones. This location of convection is optimum for the accompanying overturning circulation to concentrate absolute vorticity.

Azimuthal averaged fields derived from the Met Office regional model simulation show that the dynamics are consistent with Ooyama's classical theory for tropical cyclone intensification and its extensions that are part of the rotating-convection paradigm. In particular, the inflow is much stronger and more extensive at 1000 mb than at 850 mb, reflecting the dominance of frictionally-induced inflow. The tangential wind maximum is slightly larger also at 1000 mb, with the location of the maximum occurring at a smaller radius closer to the surface, indicating strong spin up in the friction layer, which is a consequence of the boundary layer spin up mechanism. The flow structure in the boundary layer is consistent with that described for tropical cyclones.

In summary, the rotating-convection paradigm for tropical cyclone behaviour provides an attractive framework for interpreting the dynamics of formation and intensification of this particular medicane. An alternative and currently widely accepted explanation for the intensification of medicanes, the so-called "Wind-Induced Surface Heat Exchange (WISHE) mechanism" is argued to be incomplete making it untestable. Like the proposed WISHE theory, the rotating-convection paradigm has not been fully developed to account for vortex evolution in situations where vertical wind shear is appreciable. For this reason, it may not apply to all observed cases of medicanes, especially to the many cases in which baroclinic processes appear to play a major role.

9. Acknowledgments

This study was motivated by a post that Julian Heming made to the Tropical Storms mailing list, alerting members to a forecast of the imminent occurrence of the December 2020 medicane. We thank Kevin Tory and three anonymous reviewers for their perceptive comments on the original version of the manuscript and Michael Montgomery for many stimulating discussions about the issues raised in the paper. The comments have helped us to produce what we believe is a substantially improved version.

10. Appendix 1: Interpretation of Zhang and Emanuel's example of feedback

In section 2 of their paper, Zhang and Emanuel discuss an equation of a purported feedback problem which is presumably intended to be an analogy to their envisaged WISHE feedback. In this example, they consider an air parcel is rising under its buoyancy, B, in an unstable density stratified fluid and resisted by a quadratic drag proportional to the parcel's vertical velocity, w. The *dimensional form* of the equations is

$$\frac{dw}{dt} = B - \alpha|w|w, \tag{1}$$

$$\frac{dB}{dt} = -N^2 w, \tag{2}$$

where α is some positive constant and N^2 is the Brunt-Väisälä frequency, which is assumed to be negative constant. Zhang and Emanuel offer the interpretation that (1) says that "convection is driven by buoyancy" and (2) that "convective instability results from a feedback between vertical velocity and buoyancy". However, in this problem, "convective instability" resides in the quantity N^2 and the fact that it is negative. The energy equation related to this system is

$$\frac{d}{dt}\left[\frac{1}{2}w^2 + \frac{1}{2N^2}B^2\right] = -\alpha|w|w^2, \tag{3}$$

where the first term on the left is the kinetic energy of the air parcel and the second term is its available potential energy. The term on the right of Equation (3) is negative definite and the only "source term" for the total energy: there is no obvious source analogous to surface enthalpy fluxes in the tropical cyclone problem, at least to us, and the instability residing in the negative N^2 would seem more analogous to Conditional Instability of the Second kind (CISK) than to WISHE. While the intention of this section of Zhang and Emanuel's paper might be to legitimize the use of the word "feedback" in the WISHE context, an articulation of the actual feedback explaining how the increase in surface enthalpy fluxes *feeds back* to increase in the surface wind speed is missing.

© 2021 Royal Meteorological Society

11. Appendix 2: The Met Office regional model

The forecasts are carried out using the Met Office regional model with the RAL2 middle latitude configuration developed at the Met Office (Steptoe et al. 2021). The details of the science configuration in the first Regional Atmosphere and Land model (RAL1) are described in Zhu and Smith (2020). Starting from RAL1, the main improvements of the model physics in RAL2 are as follows:

- Improvements to the treatment of lying snow, which allows the reintroduction of graupel into the precipitation reaching the surface;
- Reducing convective gustiness contribution to surface exchange (Redelsperger et al. 2000);
- Limiting drag over the ocean at high wind speeds by imposing a cap on the drag;
- Implementing the Leonard term fluxes (Moeng et al. 2010);
- Improved ice cloud fraction in mixed phase clouds (Abel et al. 2017).

The forecast model is integrated for two days with the initial condition downscaled from a global model, the Met Office Unified Model at 0300 UTC on 15 December 2020. The model has 90 vertical levels and the horizontal grid spacing is 0.036 degrees in both latitude and longitude, which is approximately 4 km in the meridional direction and a little less in the zonal direction. The forecast domain runs from approximately 15^oN to 55^oN and 10^oE to 50^oE and is covered by 1110 grid points in both horizontal directions.

References

Abel, S., I. Boutle, K. Waite, S. Fox, P. Brown, R. Cotton, G. Lloyd, T. Choularton, and K. Bower, 2017: The role of precipitation in controlling the transition from stratocumulus to cumulus clouds in a northern hemisphere cold-air outbreak. *J. Atmos. Sci.*, **74**, 2293–2314.

Bryan, G. H. and R. Rotunno, 2009: Evaluation of an analytical model for the maximum intensity of tropical cyclones. *J. Atmos. Sci.*, **66**, 3042–3060.

Carrió, D. S., V. Homar, A. Jansa, M. Picornell, and J. Campins, 2020: Diagnosis of a high-impact secondary cyclone during hymex-sop1 iop18. *Atmos. Res.*, **242**, 104983.

Carrió, D. S., V. Homar, A. Jansa, R. Romero, and M. A. Picornell, 2017: Tropicalization process of the 7 November 2014 Mediterranean cyclone: Numerical sensitivity study. *Atmos. Res.*, **197**, 300–312.

Chagnon, J. and S. Gray, 2009: Horizontal potential vorticity dipoles on the convective storm scale. *Quart. J. Roy. Meteor. Soc.*, **135**, 1392–1408.

Cioni, G., D. Cerrai, and D. Klocke, 2016: Investigating the predictability of a mediterranean tropical-like cyclone using a storm-resolving model. *Quart. Journ. Roy. Meteor. Soc.,*, **142**, 1757–1766.

Dafis, S., C. Claud, V. Kotroni, K. Lagouvardos, and J.-F. Rysman, 2020: Insight into convective evolution of mediterranean tropical-like cyclones. *Quart. J. Roy. Meteor. Soc.*, **146**, 4147–4169.

Dafis, S., J.-F. Rysman, C. Claud, and E. Flaounas, 2018: Remote sensing of deep convection within a tropical-like cyclone over the Mediterranean Sea. *Atmospheric Science Letters*, **19**, e823.

Emanuel, K., 2005: Genesis and maintenance of "Mediterranean hurricanes". *Adv. Geosciences*, **2**, 217–220.

Emanuel, K. A., 1986: An air-sea interaction theory for tropical cyclones. Part I: Steady state maintenance. *J. Atmos. Sci.*, **43**, 585–604.

Fita, L. and E. Flaounas, 2018: Medicanes as subtropical cyclones: the december 2005 case from the perspective of surface pressure tendency diagnostics and atmospheric water budget. *Quart. J. Roy. Meteor. Soc.*, **144**, 1028–1044.

Homar, V., R. Romero, D. Stensrud, C. Ramis, and S. Alonso, 2003: Numerical diagnosis of a small, quasi-tropical cyclone over the western Mediterranean: dynamical vs. boundary factors. *Quart. J. Roy. Meteor. Soc.*, **129**, 1469–1490.

Kilroy, G., R. Smith, and W. U., 2014: Tropical cyclone convection: the effects if ambient vertical and horizontal vorticity. *Quart. J. Roy. Meteor. Soc.*, **140**, 1756–1770.

Kilroy, G., R. K. Smith, and M. T. Montgomery, 2016a: Why do model tropical cyclones grow progressively in size and decay in intensity after reaching maturity? *J. Atmos. Sci.*, **73**, 487–503.

— 2017a: Tropical low formation and intensification over land as seen in ECMWF analyses. *Quart. Journ. Roy. Meteor. Soc.*, **143**, 772–784.

— 2017b: A unified view of tropical cyclogenesis and intensification. *Quart. Journ. Roy. Meteor. Soc.*, **143**, 450–462.

— 2018: The role of heating and cooling associated with ice processes on tropical cyclogenesis and intensification. *Quart. Journ. Roy. Meteor. Soc.*, **144**, 99–114.

Kilroy, G., R. K. Smith, M. T. Montgomery, B. Lynch, and C. Earl-Spurr, 2016b: A case-study of a monsoon low that formed over the sea and intensified over land as seen in ECMWF analyses. *Quart. J. Roy. Meteor. Soc.*, **142**, 2244–2255.

Lagouvardos, K., V. Kotroni, S. Nickovic, D. Jovic, and G. Kallos, 1999: Observations and model simulations of a winter sub-synoptic vortex over the central Mediterranean. *Meteorol. Appl.*, **6**, 371–383.

Marra, A. C., S. Federico, M. Montopoli, E. Avolio, L. Baldini, D. Casella, L. P. D'Adderio, S. Dietrich, P. Sanò, R. C. Torcasio, and G. Panegrossi, 2019: The precipitation structure of the Mediterranean tropical-like cyclone Numa: analysis of GPM observations and numerical weather prediction model simulations. *Remote Sensing*, **11**, 1690–.

Mazza, E., U. Ulbrich, and R. Klein, 2017: The tropical transition of the October 1996 medicane in the western Mediterranean Sea: a warm seclusion event. *Mon. Wea. Rev.*, **145**, 2575–2595.

Michaelides, S., T. Karacostas, J. L. Sánchez, A. Retalis, I. Pytharoulis, V. Homar, R. Romero, P. Zanis, C. Giannakopoulos, J. Bühl, A. Ansmann, A. Merino, P. Melcón, K. Lagouvardos, V. Kotroni, A. Bruggeman, J. I. López-Moreno, C. Berthet, E. Katragkou, F. Tymvios, D. G. Hadjimitsis, R.-E. Mamouri, and A. Nisantzi, 2018: Reviews and perspectives of high impact atmospheric processes in the Mediterranean. *Atmos. Res.*, **208**, 4–44.

Miglietta, M. M., D. Carnevale, V. Levizzani, and R. Rotunno, 2020: Role of moist and dry air advection in the development of mediterranean tropical-like cyclones (medicanes). *Quart. Journ. Roy. Meteor. Soc.*, **146**, 876–899.

Miglietta, M. M., D. Mastrangelo, and D. Conte, 2015: Influence of physics parameterization schemes on the simulation of a tropical-like cyclone in the Mediterranean Sea. *Atmos. Res.*, **153**, 360–375.

Miglietta, M. M., A. Moscatello, D. Conte, G. Mannarini, G. Lacorata, and R. Rotunno, 2011: Numerical analysis of a mediterranean 'hurricane' over south-eastern italy: sensitivity experiments to sea surface temperature. *Atmos. Res.*, **101**, 412–426.

Miglietta, M. M. and R. Rotunno, 2019: Development mechanisms for mediterranean tropical-like cyclones (medicanes). *Quart. Journ. Roy. Meteor. Soc.*, **145**, 1444–1460.

Moeng, C. H., P. P. Sullivan, M. F. Khairoutdinov, and D. A. Randall, 2010: A mixed scheme for subgrid-scale fluxes in cloud-resolving models. *J. Atmos. Sci.*, **67**, 3692–3705.

Montgomery, M. T., G. Kilroy, R. K. Smith, and N. Črnivec, 2020: Contribution of mean and eddy momentum processes to tropical cyclone intensification. *Quart. J. Roy. Meteor. Soc.*, **146**, 3101–3117.

Montgomery, M. T., S. V. Nguyen, R. K. Smith, and J. Persing, 2009: Do tropical cyclones intensify by WISHE? *Quart. Journ. Roy. Meteor. Soc.*, **135**, 1697–1714.

© 2021 Royal Meteorological Society

Montgomery, M. T., J. Persing, and R. K. Smith, 2015: Putting to rest WISHE-ful misconceptions. *J. Adv. Model. Earth Syst.*, **07**, doi:10.1002/.
Montgomery, M. T. and R. K. Smith, 2014: Paradigms for tropical cyclone intensification. *Aust. Met. Ocean. Soc. Journl.*, **64**, 37–66.
— 2017: Recent developments in the fluid dynamics of tropical cyclones. *Annu. Rev. Fluid Mech.*, **49**, 541–574.
— 2019: Toward understanding the dynamics of spinup in Emanuel's tropical cyclone model. *J. Atmos. Sci.*, **76**, 3089–3093.
Moscatello, A., M. M. Miglietta, and R. Rotunno, 2008: Numerical analysis of a Mediterranean "hurricane" over southeastern Italy. *Monthly Weather Review*, **136(11)**, 373–4397.
Muzio, E. D., M. Riemer, A. H. Fink, and M. Maier-Gerber, 2019: Assessing the predicta-bility of medicanes in ecmwf ensemble forecasts using an object-based approach. *Quart. Journ. Roy. Meteor. Soc.,*, **145**, 1202–1217.
Nolan, D., 2007: What is the trigger for tropical cyclogenesis? *Aust. Meteorol. Mag*, **56**, 241–266.
Olander, T. L. and C. S. Velden, 2009: Tropical cyclone convection and intensity analysis using differenced infrared and water vapor imagery. *Wea. Forecasting*, **24**, 1558–1572.
Ooyama, K. V., 1969: Numerical simulation of the life cycle of tropical cyclones. *J. Atmos. Sci.*, **26**, 3–40.
Persing, J., M. T. Montgomery, J. McWilliams, and R. K. Smith, 2013: Asymmetric and axisymmetric dynamics of tropical cyclones. *Atmos. Chem. Phys.*, **13**, 12299–12341.
Picornell, M. A., J. Campins, and A. Jansa, 2014: Detection and thermal description of medicanes from numerical simulation. *Natural Hazards and Earth System Sciences.*, **14**, 1059–1070.
Pytharoulis, I., G. Craig, and S. Ballard, 2000: The hurricane-like mediterranean cyclone of january 1995. *Met. Apps*, **7**, 261–279.
Pytharoulis, L., 2018: The hurricane-like Mediterranean cyclone of January 1995. *Atmos. Res.*, **208**, 261–279.
Redelsperger, J.-L., F. Guichard, and S. Mondon, 2000: A parameterization of mesoscale enhancement of surface fluxes for large-scale models. *J. Clim.*, **13**, 402–421.
Rogers, R. F., P. D. Reasor, and S. Lorsolo, 2013: Airborne doppler observations of the inner-core structural differences between intensifying and steady-state tropical cyclones. *Mon. Wea. Rev.*, **141**, 2970–2991.
Rotunno, R. and K. A. Emanuel, 1987: An air-sea interaction theory for tropical cyclones. Part II Evolutionary study using a nonhydrostatic axisymmetric numerical model. *J. Atmos. Sci.*, **44**, 542–561.
Schmetz, J., P. Pili, S. Tjemkes, D. Just, J. Kerkmann, S. Rota, and A. Ratier, 2002: An introduction to meteosat second generation (msg). *Bull. Amer. Meteorol. Soc.*, **83**, 977–992.
Smith, R., J. Zhang, and M. Montgomery., 2017: The dynamics of intensification in an hwrf simulation of hurricane earl (2010). *Quart. J. Roy. Meteor. Soc.*, **143**, 293–308.
Smith, R. K., G. Kilroy, and M. T. Montgomery, 2021: Tropical cyclone life cycle in a three-dimensional numerical simulation. *Quart. Journ. Roy. Meteor. Soc.*, **147**, submitted.
Smith, R. K. and M. T. Montgomery, 2016: The efficiency of diabatic heating and tropical cyclone intensification. *Quart. Journ. Roy. Meteor. Soc.*, **142**, 2081-2086.
Smith, R. K., M. T. Montgomery, G. Kilroy, S. Tang, and S. K. Müller, 2015: Tropical low formation during the Australian monsoon: the events of January 2013. *Aust. Met. Ocean. Soc. Journl.*, **65**, 318–341.
Smith, R. K., M. T. Montgomery, and S. V. Nguyen, 2009: Tropical cyclone spin up revisited. *Quart. Journ. Roy. Meteor. Soc.*, **135**, 1321–1335.
Smith, R. K., M. T. Montgomery, and S. Vogl, 2008: A critique of Emanuel's hurricane model and potential intensity theory. *Quart. Journ. Roy. Meteor. Soc.*, **134**, 551–561.
Steptoe, H., N. Savage, S. Sadri, K. Salmon, Z. Maalick, and S. Webster, 2021: Tropical cyclone simulations over bangladesh at convection permitting 4.4 km and 1.5 km resolution, scientific data. *Nature*, http://doi.org/10.1038/s41597-021-00847-5.
Tous, M. and R. Romero, 2011: Medicanes: cataloguing criteria and exploration of meteorological environments. *Tethys*, **8**, 53–61.
— 2013: Meteorological environments associated with medicane development. *Int. J. Climatol.*, **33**, 1–14.
von Storch, L. C. H. and S. Gualdi, 2014: A long-term climatology of medicanes. *Clim Dyn*, **43**, 1183–1195.
Weijenborg, C., P. Chagnon, J.M. abd Friederichs, S. Gray, and A. Hense, 2017: Coherent evolution of potential vorticity anomalies associated with deep moist convection. *Quart. J. Roy. Meteor. Soc.*, **143**, 1254–1267.
Zhang, F. and K. A. Emanuel, 2016: On the role of surface fluxes and WISHE in tropical cyclone intensification. *J. Atmos. Sci.*, **73**, 2011–2019.
Zhu, H. and R. K. Smith, 2020: A case-study of a tropical low over northern australia. *Quart. Journ. Roy. Meteor. Soc.*, **146**, 1702–1718.

© 2021 Royal Meteorological Society